

Electronic Supplementary Information (ESI)
Microrod Crystals Formed via Rhein Molecules-Mediated
Mineralization

Jiaying Liu,^{a, b} Zhenyan Zhang,^a Yu Yan,^{a, b} Xiaonong Zhang,^b Chunsheng Xiao^{*a, b} and
Xuesi Chen^{*a, b}

^a School of Applied Chemistry and Engineering, University of Science and Technology
of China, Hefei, Anhui 230026, China

E-mail: xschen@ciac.ac.cn, xiaocs@ciac.ac.cn

^b Key Laboratory of Polymer Ecomaterials, Changchun Institute of Applied Chemistry,
Chinese Academy of Sciences, Changchun 130022, China

E-mail: xschen@ciac.ac.cn, xiaocs@ciac.ac.cn

Experimental

1. Materials

High molecular weight sodium hyaluronate (H-HA, $M_w = 2,000$ kDa) and low molecular weight sodium hyaluronate (L-HA, $M_w = 3$ kDa) were purchased from Shanghai yuanye Bio-Technology Co., Ltd. Rhein (Rhe) were purchased from Shanghai Macklin Biochemical Co., Ltd. Dulbecco's modified eagle medium (DMEM), heat-inactivated fetal bovine serum, streptomycin, and penicillin were purchased from servicebio. Co., Ltd. The mouse embryonic osteoblasts (MC3T3 fibroblast), mouse fibroblast (L929 fibroblast), and mouse mononuclear macrophages cells (RAW264.7 cells) were purchased from BeNa Culture Collection (Beijing, China). 2',7'-Dichlorofluorescein diacetate (DCFH-DA) was purchased from Shanghai D&B Biochemical Co., Ltd. TNF- α ELISA kits and IL-6 ELISA kits were purchased from Thermo Fisher Scientific (China) Co., Ltd. All the other reagents and solvents were purchased from Sinopharm Chemical reagent Co., Ltd., China and used as obtained.

2. Methods

2.1 Preparation of H-HA-stabilized Rhe-mineralized microrods (H-RMM)

50 mg of H-HA and 12 mg of Rhe were dissolved in 10 mL of deionized (DI) water. Then 24 μL of 500 mg mL^{-1} CaCl_2 was dropped into the above system at 30 °C. After that, the mixture was stirred at 30 °C for 18 h and subsequently incubated at 37 °C for 9 d. The H-RMM was obtained by centrifugation (5000 rpm, 5 min), washing thrice with DI water and lyophilization.

2.2 Preparation of Rhe-Ca

12 mg of Rhe, 24 μL of 500 mg mL^{-1} CaCl_2 , and 25 μL NaOH (100 mg mL^{-1}) were mixed into 5 mL of DI water. After that, the mixture was stirred at 30 $^\circ\text{C}$ for 18 h and subsequently incubated at 37 $^\circ\text{C}$ for 9 d. The Rhe-Ca was obtained by centrifugation (5000 rpm, 5 min), washing thrice with DI water and lyophilization.

2.3 Preparation of L-HA-stabilized Rhe-mineralized microrods (L-RMM)

50 mg of L-HA(HA3K) and 12 mg of Rhe were dissolved in 10 mL of DI water. Then, 24 μL of 500 mg mL^{-1} CaCl_2 was dropped into the above system. The obtained mixture was stirred at 30 $^\circ\text{C}$ for 18 h and subsequently incubated at 37 $^\circ\text{C}$ for 9 d. The L-RMM was obtained by centrifugation (5000 rpm, 5 min), washing thrice with DI water and lyophilization.

2.4 Scanning electron microscope (SEM) characterization

Rhe, Rhe-Ca, L-RMM, and H-RMM were dissolved or suspended in DI water. 10 μL of samples was dropped into silicon slices. After drying at room temperature, the morphologies of samples were observed by a SEM (Zeiss Merlin, Germany).

2.5 Different components contents in RMMs

To measure the Rhe contents in RMMs, Rhe was firstly dissolved into NaOH solution with $\text{pH} = 10$. Then, UV/vis spectra were recorded on a PDA UV/Vis spectrophotometry (Lambda 265, PerkinElmer, USA), and absorbance values from 200 to 700 nm were recorded. The absorbance values of Rhe with various concentrations at 251 nm were used to fabricate the standard curve. Next, UV/Vis spectra of Rhe, Rhe-Ca, L-RMM, and H-RMM dissolved into NaOH solution were measured at the concentrations of 16, 32, 64, and 128 $\mu\text{g mL}^{-1}$. Finally, Rhe contents in RMMs were

calculated by comparing their absorbance values at 251 nm to the standard curve.

Ca ions contents in RMMs were detected by inductively coupled plasma mass spectrometry (ICP MS, Thermo Scientific™ ICAP™ 7400 ICP, Thermo Fisher Scientific-Shanghai, China).

2.6 Atomic force microscopy characterization (AFM)

The thickness and typical mechanical properties of RMMs at nano level were examined using an atomic force microscopy (Dimension ICON, Bruker, German). Examination was performed in the bimodal amplitude-frequency-modulated (AM-FM) imaging mode to determine the young's modulus (modulus of elasticity). NanoScope Analysis 1.9 software was used to analyze the acquired images.

2.7 Fourier transform infrared (FT-IR) spectroscopy

FT-IR spectra were recorded with a Fourier Transform Infrared Spectrometer (INVENIO-R, Bruker, German) and scanned between 4000 and 400 cm^{-1} .

2.8 Fluorescence spectroscopy

Fluorescence spectrum was recorded on a Spark™ Multimode microplate reader (Tecan, Switzerland) in a 96-well plate. The 100 μL of Rhe, Rhe-Ca, L-RMM, and H-RMM were detected at the concentration of 128 μM . Samples were excited at 450 nm, monitoring the emission from 500 to 800 nm.

2.9 X-ray diffraction characterization (XRD)

XRD measurements were carried out on a goniometer (D8 ADVANCE, Bruker, German) with an X-ray of $\lambda = 1.54 \text{ \AA}$, operated at 40 kV and 40 mA. Data was collected for 2θ from 5° to 70° with the step-size at 0.050134.

2.10 X-ray photoelectron spectroscopy (XPS)

X-ray photoelectron spectroscopy (XPS) measurements were carried out on a goniometer (ESCALAB 250Xi, Thermo, USA) with Al K Alpha, operated at 20.0 eV. Data was collected for the spot size of 500 μm with the step-size at 0.05 eV.

2.11 In vitro drug release behavior

1 mL of PBS buffer with a pH of 7.4, containing either 2 mg of Rhe or RMMs, was subjected to dialysis using dialysis membranes (1 kDa MWCO). The dialysis was carried out against 9 mL of PBS buffer at 37 °C. At specified time intervals, 1 mL of PBS was collected and replenished with an equal volume of fresh PBS. The absorbance of the collected PBS was then measured from 200 to 800 nm using a PDA UV/Vis spectrophotometry (Lambda 265, PerkinElmer, USA). The absorbance values at 255 nm for the Rhe at different concentrations were used to generate a standard curve. The cumulative amount of Rhe released from Rhe or RMMs was calculated using the above standard curve.

2.12 Hemolysis assay

For blood compatibility of Rhe and RMMs, 2 v/v % red blood cells suspensions were co-incubated with various mass samples at 37 °C. 2 v/v % red blood cells suspensions were respectively co-incubated with PBS and DI water as negative and positive groups. After 3 h of co-incubation, the mixture solution was centrifugated (1500 rpm, 10 min) and visualization supernatants condition of all samples were obtained by a camera. Then, 200 μL of the supernatant was extracted and added to a 96-well plate. The UV absorbance intensity was obtained by measuring values at OD 545 nm using an

ultraviolet-visible spectrophotometer (Spark™ Multimode microplate reader, Tecan, Switzerland). All samples were measured four times. Finally, the morphology of RBCs was observed by under optical microscopy.

2.13 Cytotoxicity assay

Cell viabilities were assessed in the L929, MC3T3 fibroblast and RAW264.7 cells lines using the cell counting kit-8 (CCK-8) method. 1×10^4 of L929 or MC3T3 fibroblasts were seeded in each well of a 96-well cell plate and incubated at 37 °C at a CO₂ cell incubator. For RAW264.7 cells, 2×10^4 cells were seeded in each well of a 96-well cell plate and incubated at 37 °C at a CO₂ cell incubator. After 24 h of cultivation, the culture medias were replaced with fresh culture medium containing various concentrations of Rhe or H-RMM. Fresh culture medium was used to culture cells as a negative group. After co-cultivation at 37 °C for 24 h, the above media was all replaced with 10 v/v% of CCK-8 media at each time point and subsequently incubated at 37 °C for 2 h. The UV absorbance intensity was obtained by measuring values at OD values of 450 nm using an ultraviolet-visible spectrophotometer (Spark™ Multimode microplate reader, Tecan, Switzerland). All samples were measured four times.

2.14 The intracellular ROS scavenging assay in LPS-stimulated RAW264.7 cell

The intracellular ROS scavenging assay was assessed in the LPS-stimulated RAW264.7 cells using the DCFH-DA staining method. 12×10^4 of RAW264.7 cells were seeded in each well of a 48-well cell plate and incubated at 37 °C at a CO₂ cell incubator. After 24 h of cultivation, RAW264.7 cells were pretreated with 20 μM of Rhe or H-RMM for 2 h and then stimulated with LPS ($1 \mu\text{g mL}^{-1}$). Fresh culture medium or LPS

(1 $\mu\text{g mL}^{-1}$) without samples were respectively used to culture cells as control or LPS groups. After co-cultivation at 37 °C for 24 h, the medium was removed and the cells were washed twice with PBS. Then, 200 μL of DCFH-DA (10 μM) was added into each well. After incubation at 37 °C for 20 min, the medium was removed, and the cells were washed twice with PBS to remove free DCFH-DA and subsequently added 100 μL PBS. The fluorescence intensity was tested by fluorescence spectrometer (Spark™ Multimode microplate reader, Tecan, Switzerland) at the excitation of 488 nm and the emission of 525 nm. All samples were measured three times.

2.15 Proinflammatory mediators (TNF- α and IL-6) scavenging assay in LPS-stimulated RAW264.7 cell

The TNF- α and IL-6 proteins expressions in LPS-stimulated RAW264.7 cell were assayed using ELISA kits. Firstly, 50×10^4 of RAW264.7 cells were seeded in each well of a 6-well cell plate and incubated at 37 °C. After 24 h of cultivation, RAW264.7 cells were pretreated with 20 μM of Rhe or H-RMM for 2 h and then stimulated with LPS (1 $\mu\text{g mL}^{-1}$) for 24 h at 37 °C. The relevant proteins expressions in the supernatants were tested using ELISA kits according to standard instructions. Fresh culture medium or LPS (1 $\mu\text{g mL}^{-1}$) without treatment were used as the negative control and positive control, respectively. The concentrations of relevant proteins were calculated from the corresponded standard curves.

2.16 Fluorescence microscopy

50×10^4 of RAW264.7 cells were seeded in each well of a 6-well cell plate and incubated at 37 °C. After 24 h of cultivation, RAW264.7 cells were treated with DMEM

mediums containing 20 μM of Rhe or H-RMM for 24 h at 37 °C. Then, the DMEM mediums were removed, and the cells were washed twice with 2 mL of PBS. We recorded the images by fluorescence microscopy (ECLIPSE Ti-S, Nikon, Japan) under blue excitation channel.

2.17 The intracellular ROS scavenging assay in H₂O₂-stimulated L929 and MC3T3 fibroblast cells lines assay

The intracellular ROS scavenging assay was assessed in the L929 and MC3T3 fibroblast cells lines using DCFH-DA staining method. 20×10^4 of L929 or MC3T3 fibroblasts were seeded in each well of a 12-well cell plate and incubated at 37 °C at a CO₂ cell incubator. After 24 h of cultivation, the culture medias were replaced with fresh culture medium containing H₂O₂ (500 μM) in the absence or presence of 20 μM of Rhe or H-RMM. Fresh culture mediums were used to culture cells as a negative group. After co-cultivation at 37 °C for 6 h, the mediums were removed and the cells were washed twice with DMEM. Then, 500 μL of 10 μM DCFH-DA was added into each well. After incubation at 37 °C for 20 min, the medium was removed, and washed twice with DMEM to remove free DCFH-DA and subsequently added 500 μL PBS. The fluorescence intensity was observed by fluorescence microscope (ECLIPSE Ti-S, Nikon, Japan) under blue excitation channel.

2.18 The protection capability of RMMs for normal cells in an excessive ROS environment assay

The Cell viabilities in an excessive ROS environment assay were assessed in the H₂O₂-induced L929 and MC3T3 fibroblast cells lines using CCK8 method. 1×10^4 of

L929 or MC3T3 fibroblasts were seeded in each well of a 96-well cell plate and incubated at 37 °C at a CO₂ cell incubator. After 24 h of cultivation, the culture medias were replaced with fresh culture medium containing H₂O₂ (500 μM) in the absence or presence of 20 μM of Rhe or H-RMM. Cells cultured with fresh culture mediums were used as the control group. After co-cultivation at 37 °C for 6 h, the above medias were all replaced with 10 v/v% of CCK-8 media and subsequently incubated at 37 °C for 2 h. 10 v/v% of CCK-8 media without cells was used as a blank group. The UV absorbance intensity was obtained by measuring values at 450 nm using a Spark™ Multimode microplate reader (Tecan, Switzerland). All samples were measured three times.

2.19 Statistical analysis

All experiments were measured in parallel at least three times. All quantitative data were expressed as mean ± SD. Multiple *t* tests method was used to analyze quantitative data. Normality and equality of variance were tested before a statistical test. **p* < 0.05 was considered possessing significant.

H-RMM

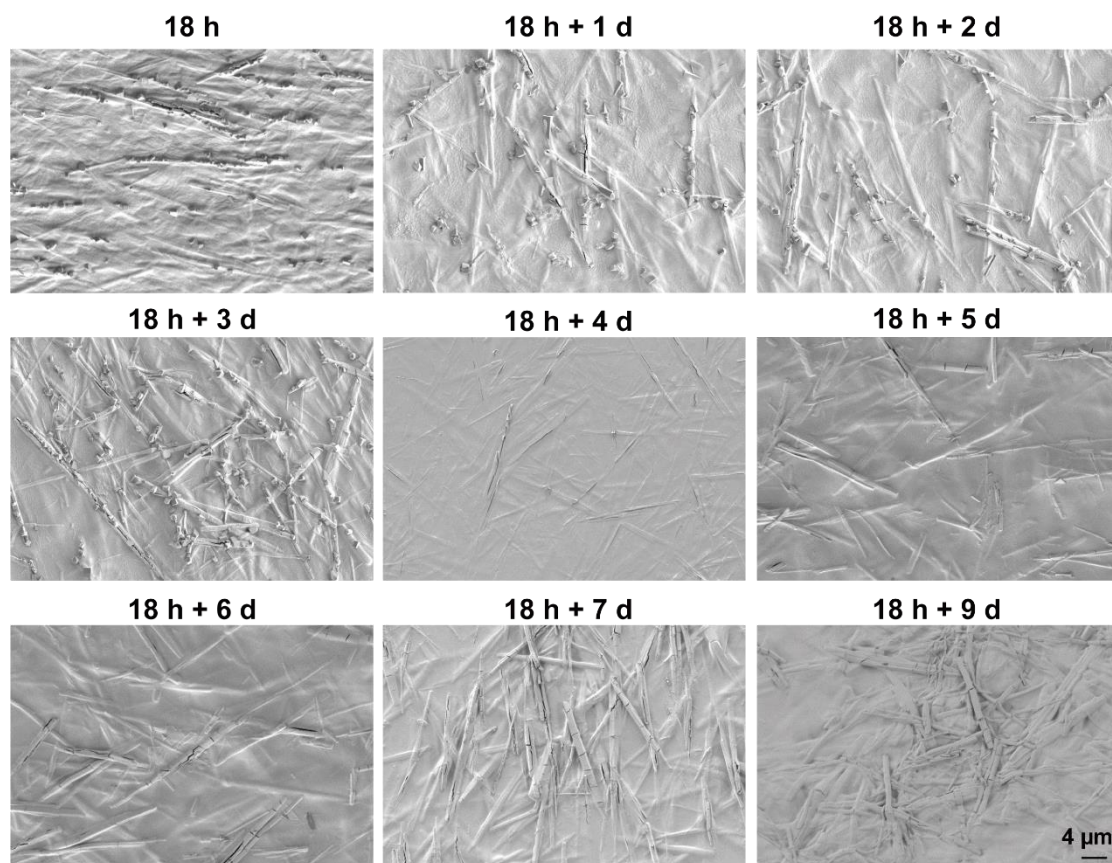


Fig. S1 SEM images of mixed solution for H-RMM during incubation at 37 °C.

Rhe

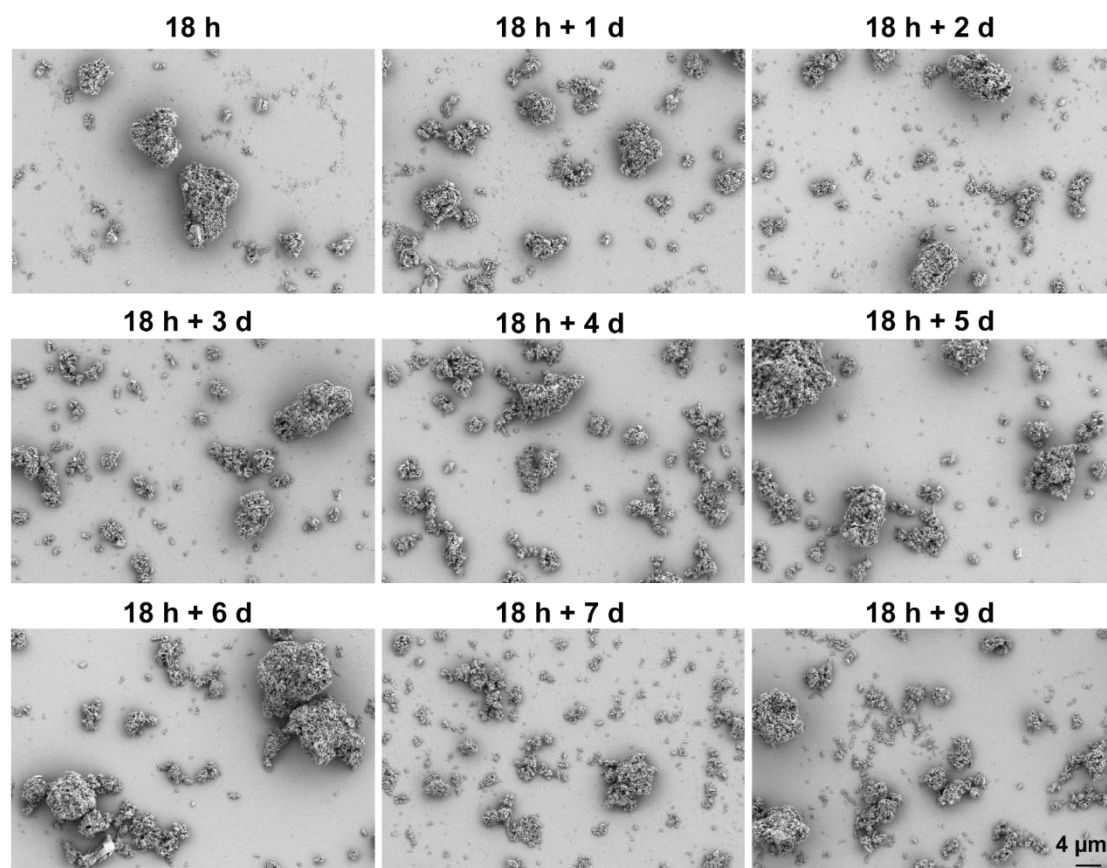


Fig. S2 SEM images of Rhe solution during incubation at 37 °C.

Rhe-Ca

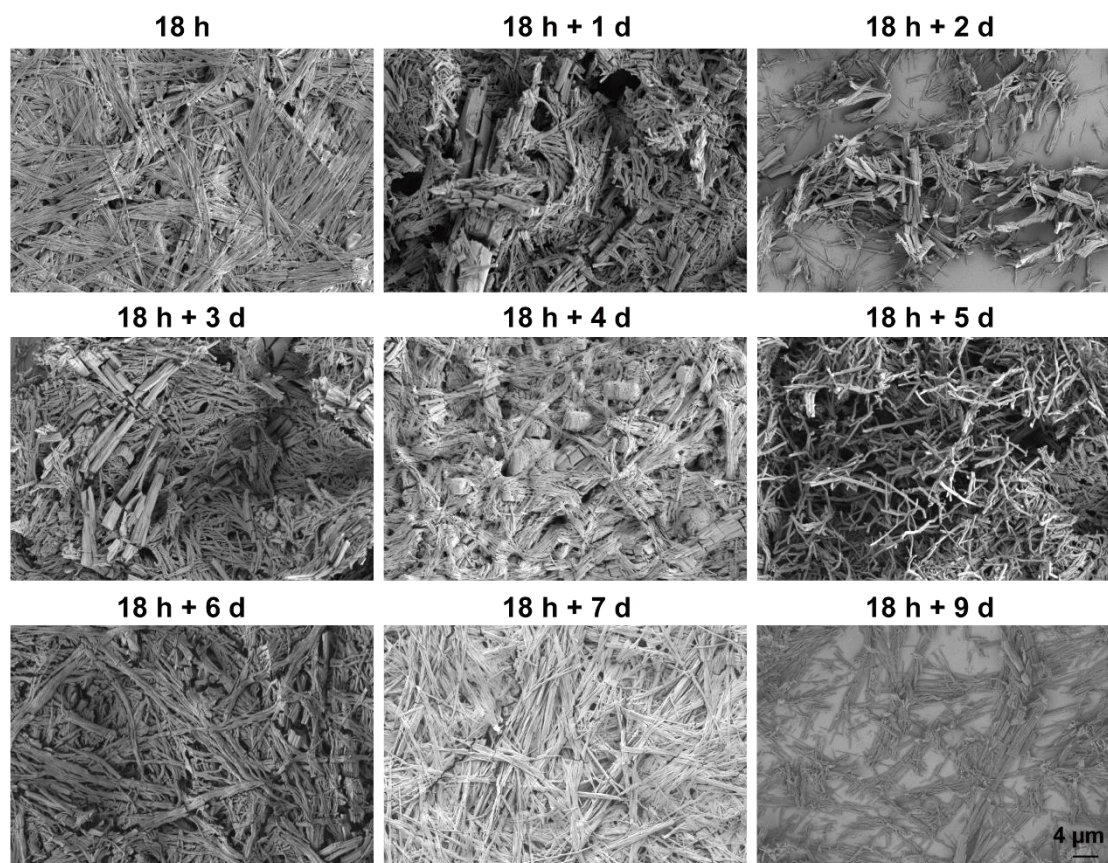


Fig. S3 SEM images of mixed solution for Rhe-Ca during incubation at 37 °C.

L-RMM

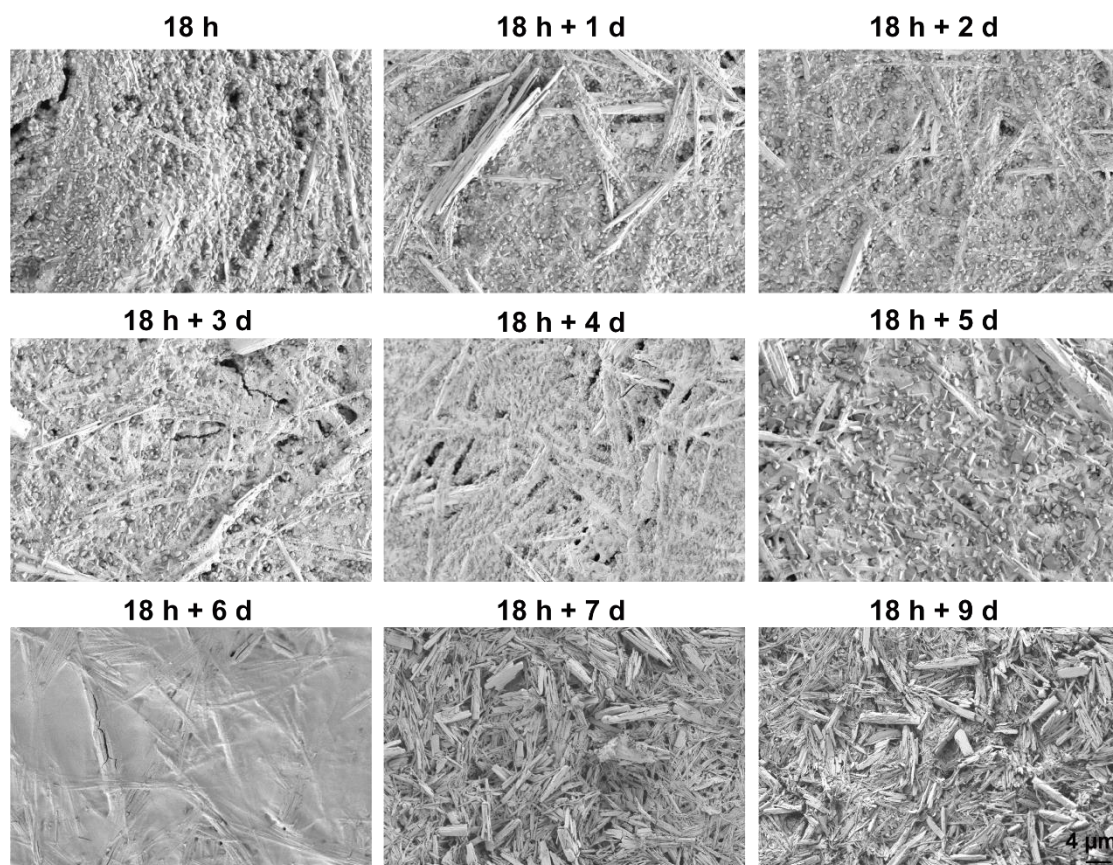


Fig. S4 SEM images of mixed solution for L-RMM during incubation at 37 °C.

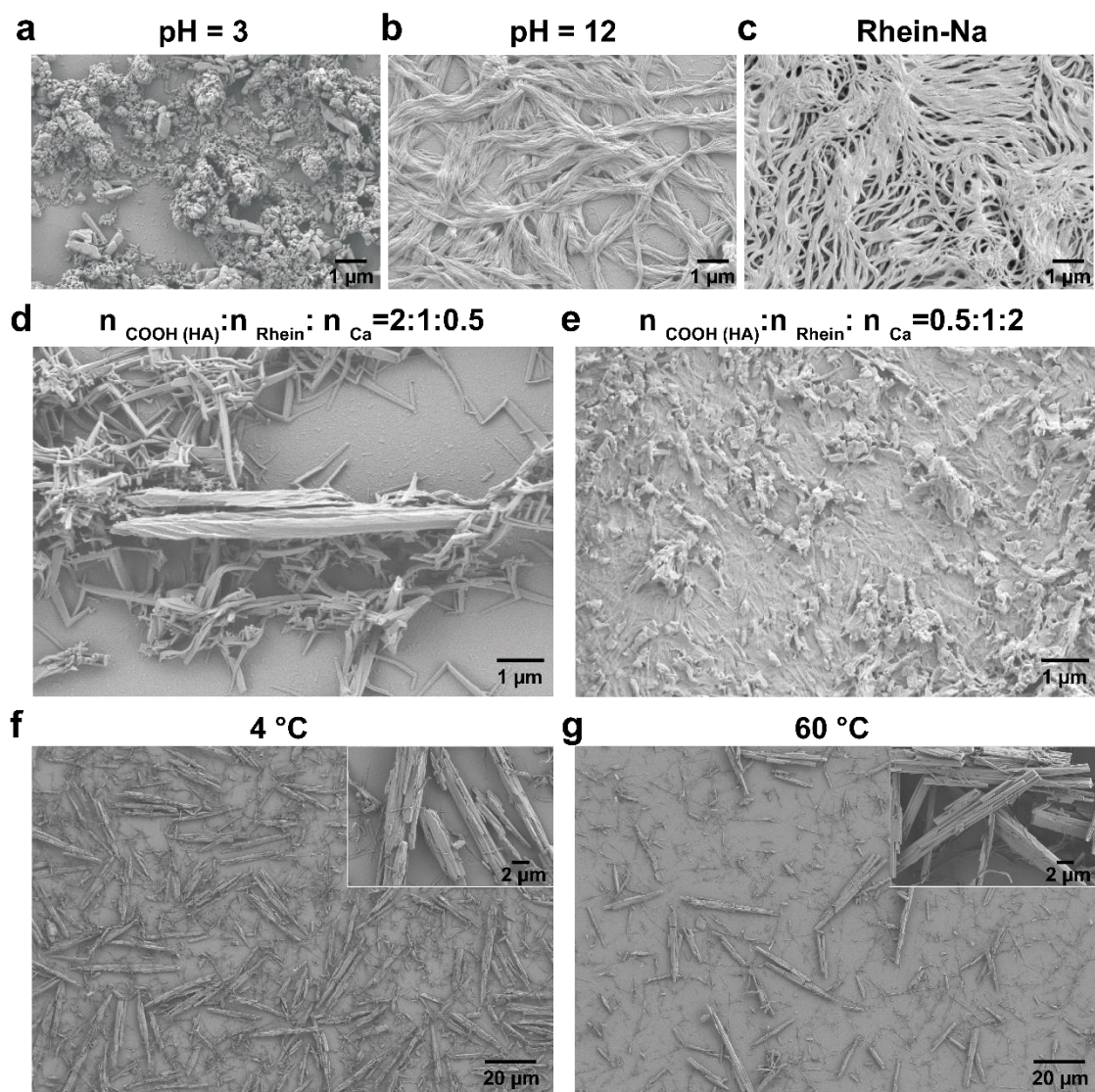


Fig. S5 a) SEM images of Rhe-mineralized samples at pH=3, b) SEM images of Rhe-mineralized samples at pH=12, c) SEM images of Rhein-Na (Rhein in NaOH solution). d) SEM images of the obtained Rhe-mineralized samples in molar ratio of 2:1:0.5 between carboxyl groups in HA chain, Rhein, and Ca ions (the decrease of Ca ion concentration), e) SEM images of the obtained Rhe-mineralized samples in molar ratio of 0.5:1:2 between carboxyl groups in HA chain, Rhein, and Ca ions (reduction of HA concentration). f) SEM images of Rhe-mineralized samples after being incubated for 9 d at 4 °C, g) SEM images of Rhe-mineralized samples after being incubated for 9 d at 60 °C.

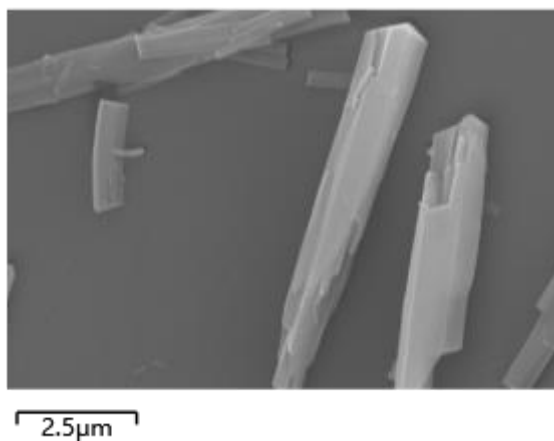


Fig. S6 SEM image of H-RMM, which is corresponding to the energy dispersive element mapping images shown in Fig 3a.

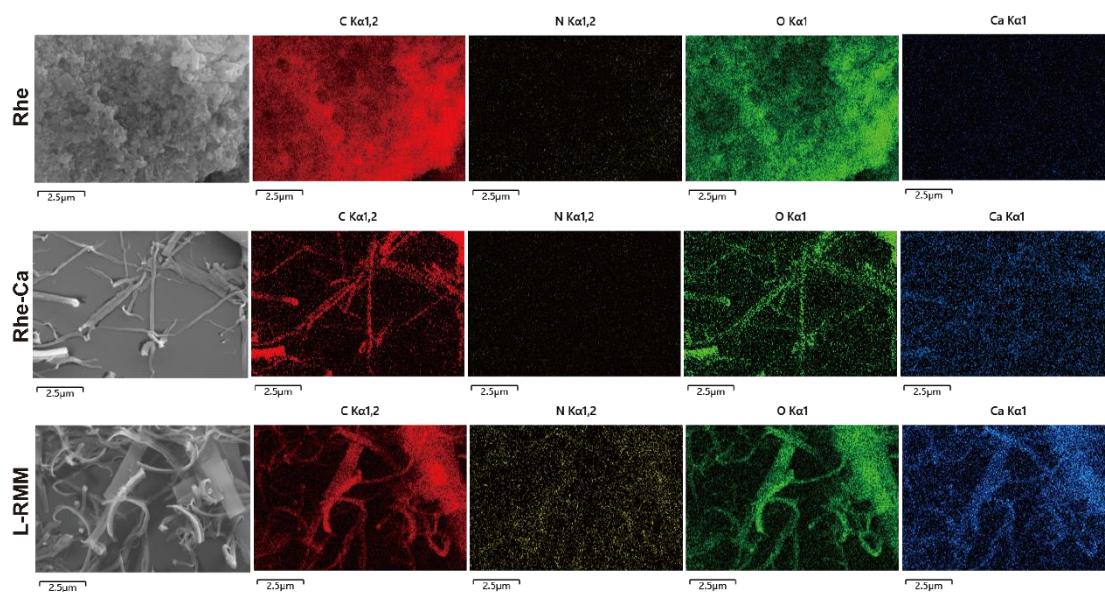


Fig. S7 Energy dispersive element mapping and corresponded SEM image of Rhe, Rhe-Ca, and L-RMM.

Table S1. Quantitative compositions analysis of Rhe-Ca, L-RMM, and H-RMM

RMMs	Rhein (wt.%)	Ca ions (wt.%)	HA (wt.%)
Rhe-Ca	72.6	26.7	/
L-RMM	80.9	12.0	7.1
H-RMM	77.1	12.0	10.7

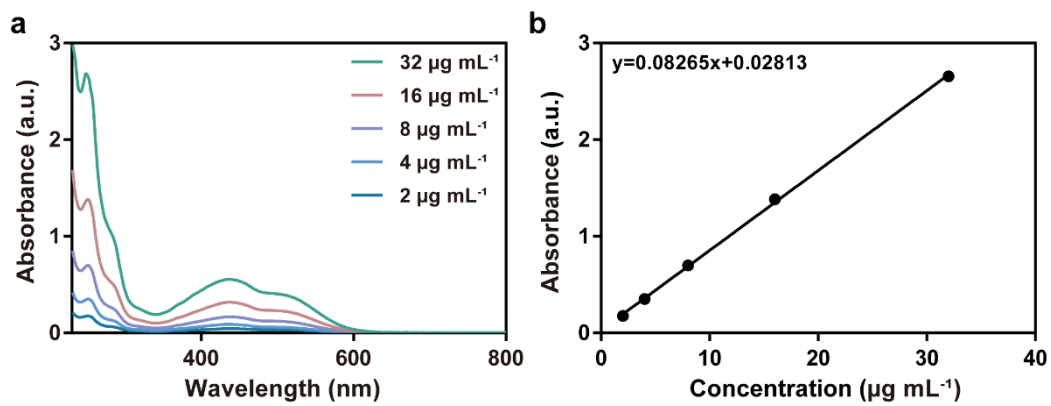


Fig. S8 a) UV/vis absorbance of dissolved Rhein at various concentration from 200 to 800 nm, b) The standard curve of dissolved Rhein at OD₂₅₁ nm.

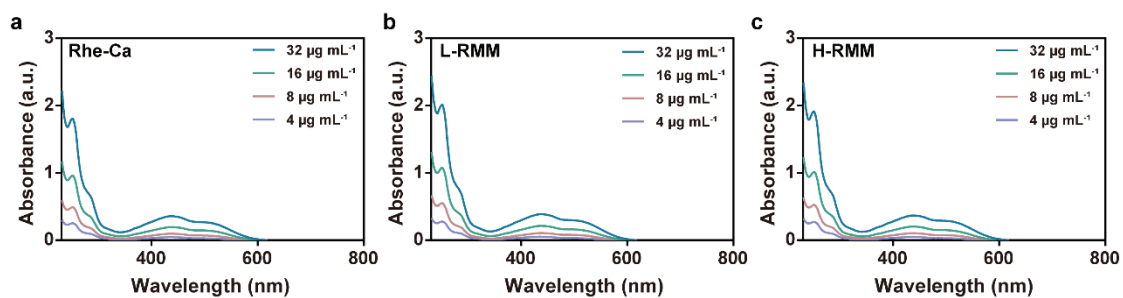


Fig. S9 UV/vis absorbance of a) dissolved Rhe-Ca, b) dissolved L-RMM, and c) dissolved H-RMM at various concentration from 200 to 700 nm. Finally, the Rhein loading efficiency in Rhe-Ca, L-RMM, and H-RMM was calculated about 72.62%, 80.90% and 77.11% by intensity values of dissolved H-RMM and the standard curve of dissolved Rhein at OD = 251 nm (Fig. S8).

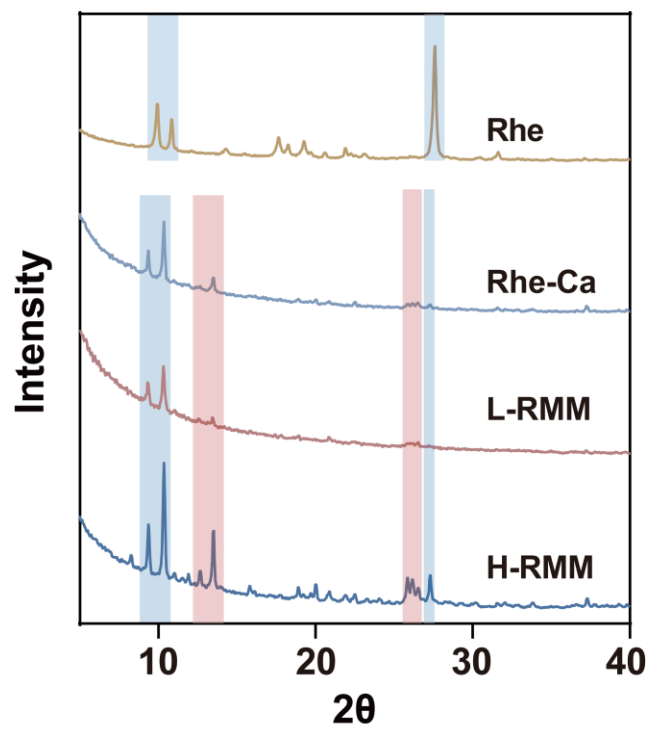


Fig. S10 X-ray diffraction spectra of Rhe, Rhe-Ca, L-RMM, and H-RMM

Table S2 Statistic 2θ and Å data of Rhe, Rhe-Ca, L-RMM, and H-RMM.

Samples	Diffraction angle 2θ (°)					
	(Interplanar crystal spacing, Å)					
Rhe	9.94	10.84				27.58
	(8.93)	(8.19)				(3.33)
Rhe-Ca	9.38	10.36				
	(9.44)	(8.55)				
L-RMM	9.38	10.36	12.66	13.51		
	(9.44)	(8.55)	(7.03)	(6.59)		
H-RMM	9.38	10.36	12.66	13.51	26.5	27.29
	(9.44)	(8.55)	(7.03)	(6.59)	(3.45)	(3.36)

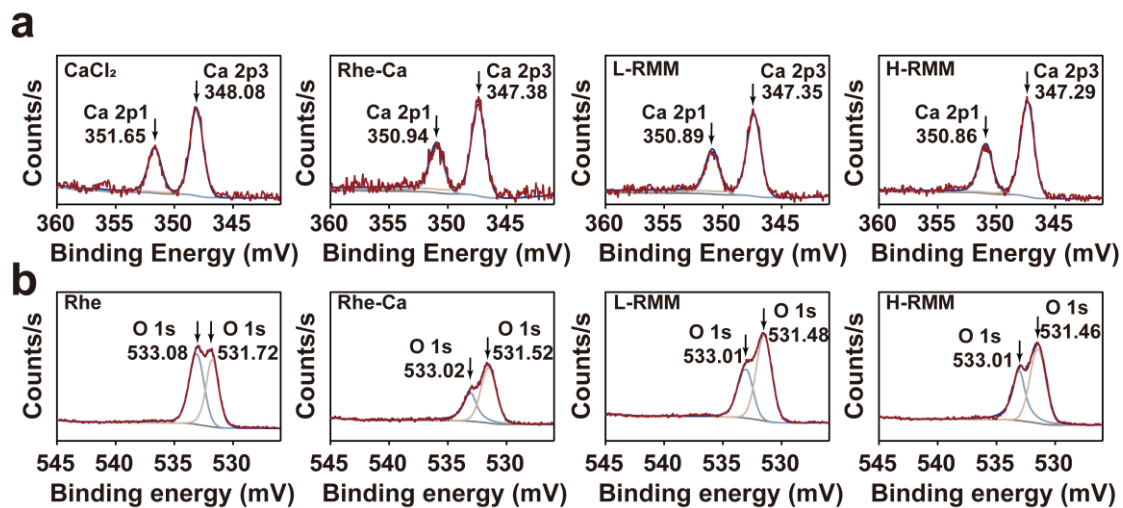


Fig. S11 a) XPS spectra of Ca 2p from CaCl₂, Rhe-Ca, L-RMM, and H-RMM, b) XPS spectra of O 1s from Rhe, Rhe-Ca, L-RMM, and H-RMM.

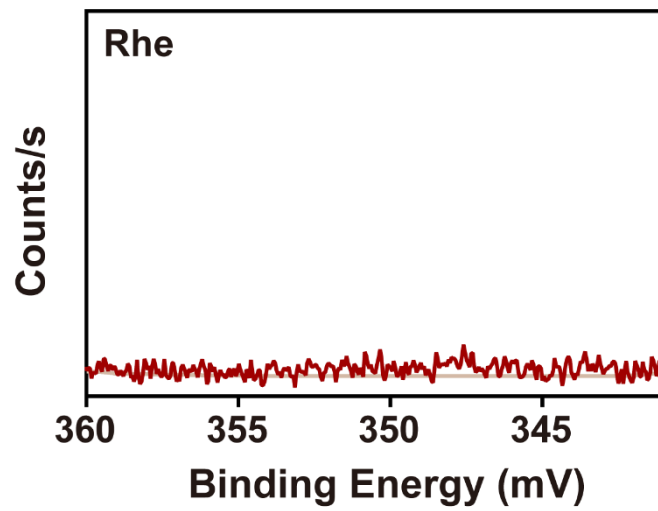


Fig. S12 XPS spectra of Ca 2p in Rhe.

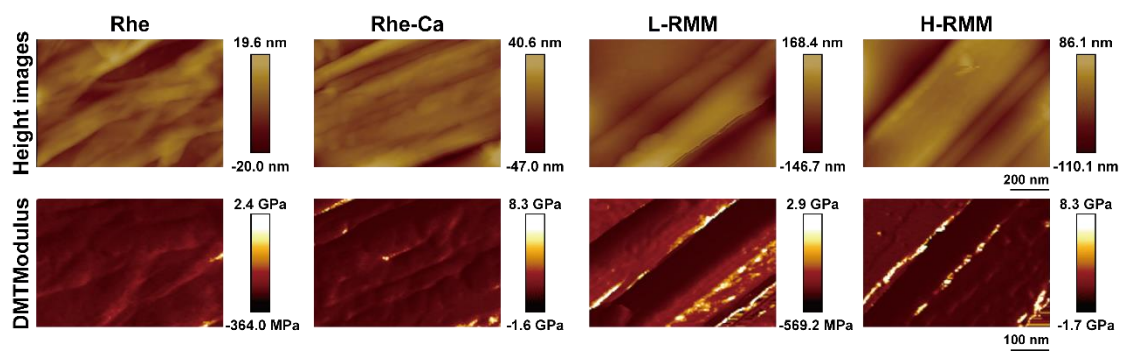


Fig. S13 Height images and DMT Modulus images of Rhe, Rhe-Ca, L-RMM, and H-RMM.

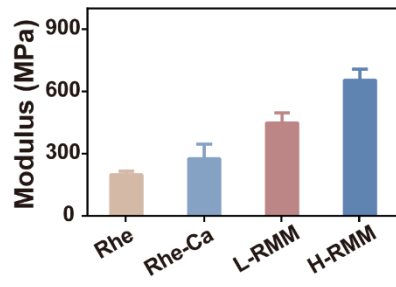


Fig. S14 Young's modulus of Rhe, Rhe-Ca, L-RMM, and H-RMM.

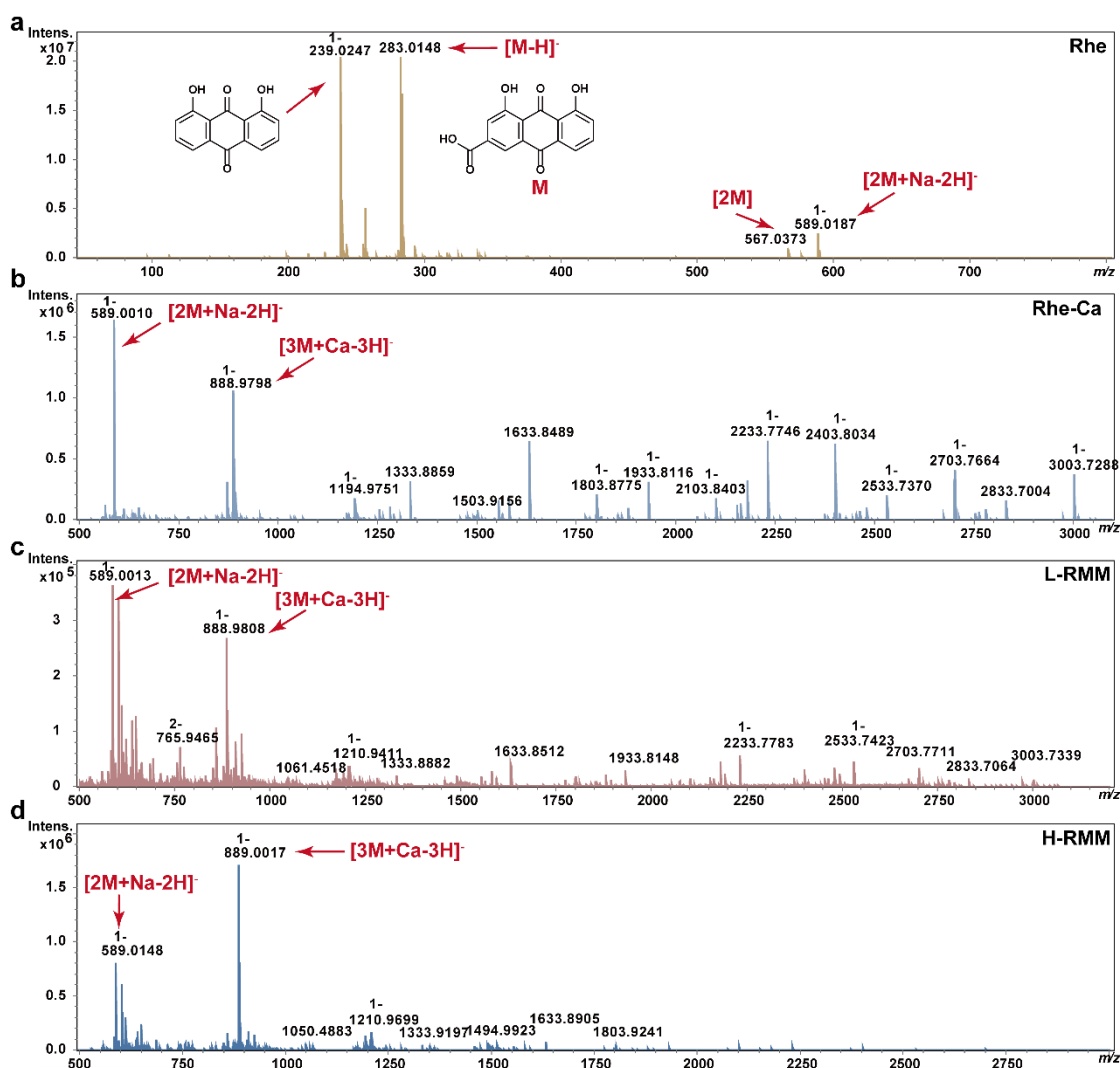


Fig. S15 Mass spectrometric analysis of a) free Rhe, b) Rhe-Ca, c) L-RMM, and d) H-RMM. Free Rhe was mainly composed of the monomers $[M-H]^-$ (m/z 239.0214 and 283.0095) (a). In contrast, the dimers (m/z 589.0148), trimers (m/z 889.007), and higher-order aggregates were observed in Rhe-Ca, L-RMM and H-RMM (b-e). These aggregates existed as Rhe-metal clusters, the dimers $[2M+Na-2H]^-$ were the main aggregated clusters in Rhe-Ca and L-RMM, indicating that the dimer was relatively stable compared with other aggregates (b, c). Notably, the predominant aggregated clusters in H-RMM were the trimers $[3M+Ca-2H]^-$ (d), demonstrating higher degrees of Rhe aggregates in H-RMM relative to Rhe-Ca and L-RMM.^{1,2}

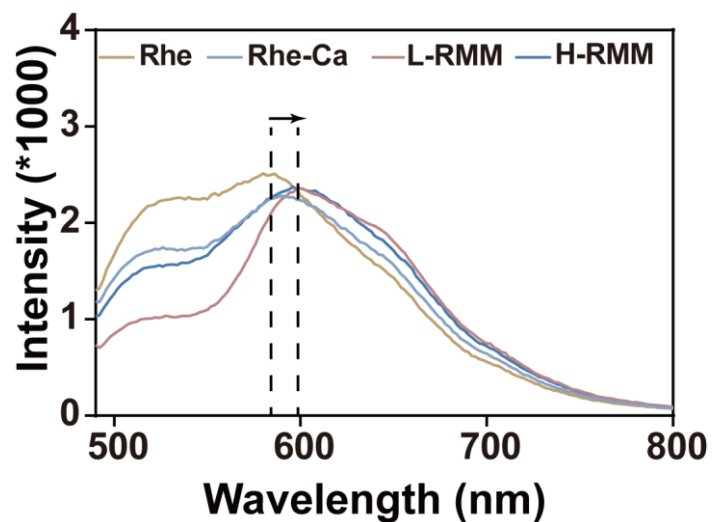


Fig. S16 Fluorescence spectra of Rhe, Rhe-Ca, L-RMM, and H-RMM. Fluorescence spectroscopy results displayed a characteristic emission peak from free Rhe at 601 nm shifted toward 616 nm at L-RMM and H-RMM due to the Rhe aggregated by π - π interactions. And the aggregated Rhe in RMMs also caused the characteristic peak intensity to decrease owing to fluorescence tendency quench.³

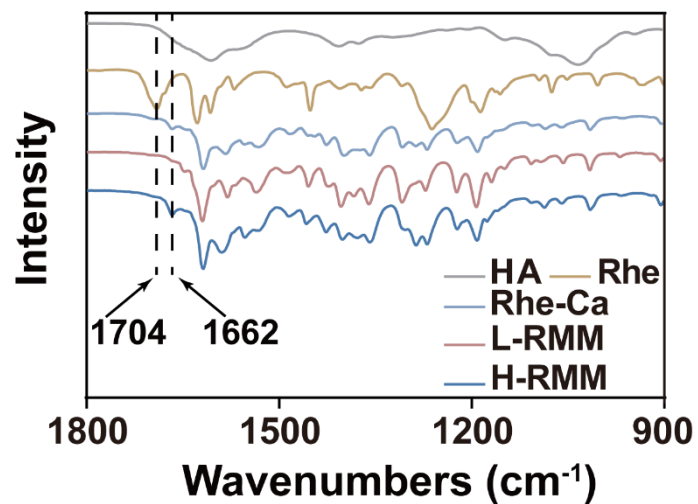


Fig. S17 FT-IR from 1800 cm⁻¹ to 900 cm⁻¹ of HA, Rhe, Rhe-Ca, L-RMM, and H-RMM.

The peak of C=O at 1704 cm⁻¹ from Rhe shifted to 1662 cm⁻¹ after mineralization at Rhe-Ca, L-RMM, and H-RMM, indicating that hydrogen bonds were involved in the mineralization process.⁴

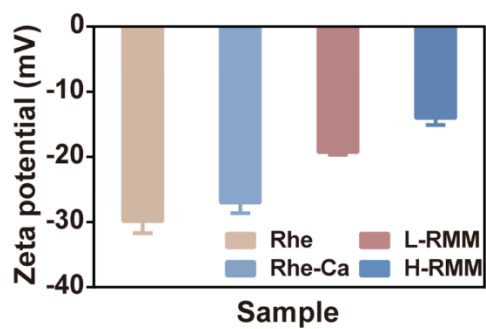


Fig. S18 Zeta potential of Rhe, Rhe-Ca, L-RMM, and H-RMM. The diminished negative charge for H-RMM should be ascribed to the the aggregation of highly-charged Rhe-Ca and HA into dense microrod structure, which is consistent with previous report.⁵

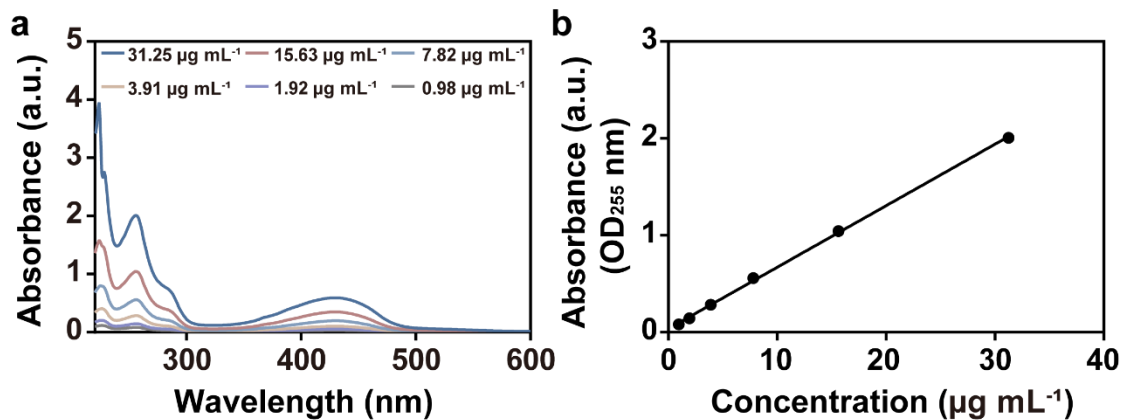


Fig. S19 a) UV/vis absorbance of Rhe in PBS (pH = 7.4) at various concentration from 200 to 700 nm, b) The standard curve of Rhe at OD₂₅

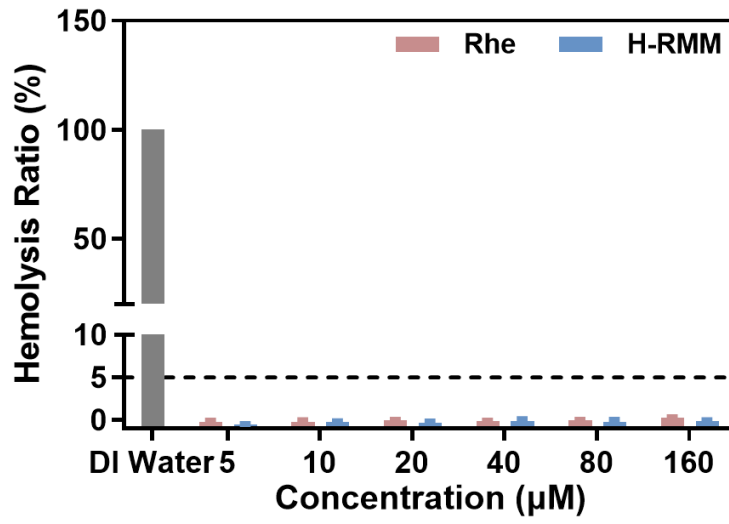


Fig. S20 Hemolysis assay of Rhe and H-RMM.

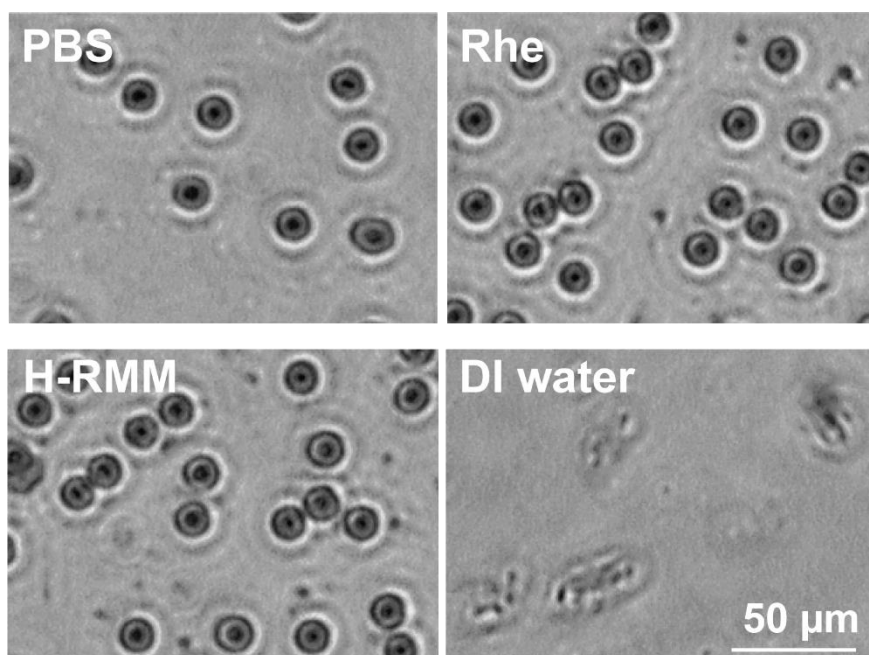


Fig. S21 Image of RBCs after treatment with PBS, Rhe, H-RMM or DI water.

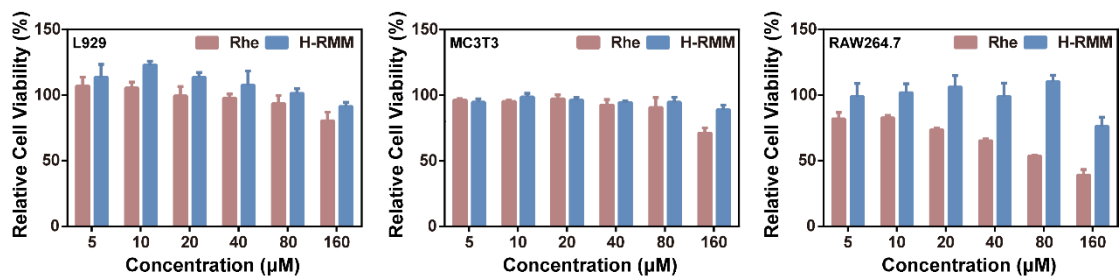


Fig. S22 Relative cell viability of Rhe and H-RMM after 24 h of co-incubation with L929, MC3T3, and RAW264.7 cells.

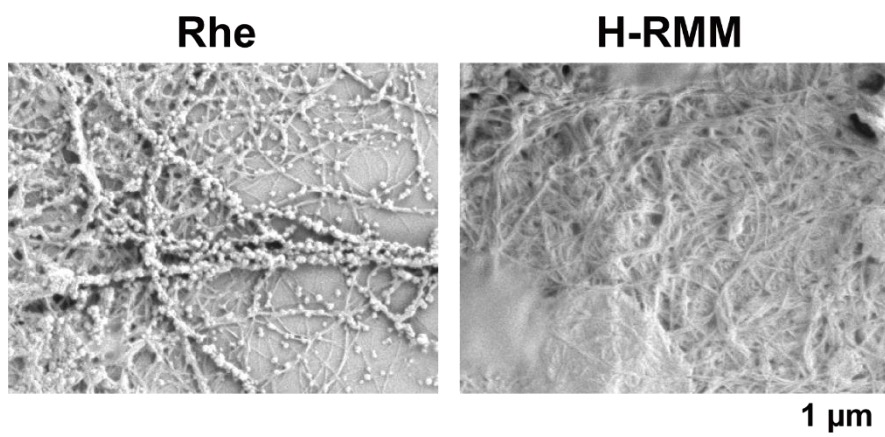


Fig. S23 The representative morphologies of Rhe released from Rhe or H-RMM at 37 °C for 24 h.

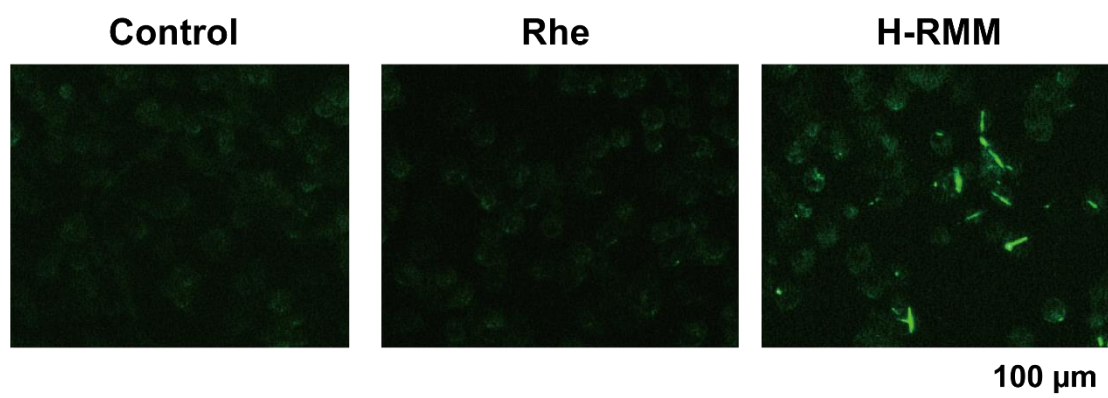


Fig. S24 Fluorescent images (green fluorescence from Rhe) of RAW264.7 cells co-incubated with 20 μM of Rhe or H-RMM at 37 $^{\circ}\text{C}$ for 24 h.⁶

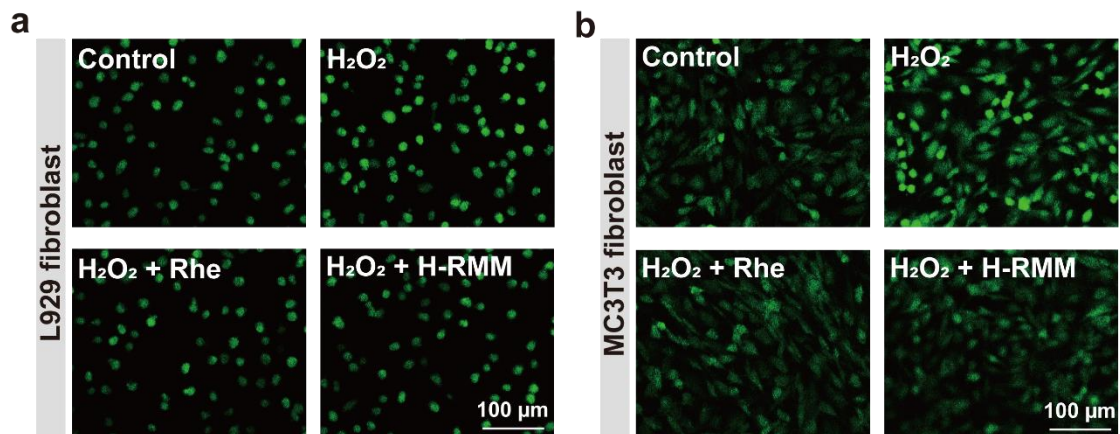


Fig. S25 Fluorescence images of intracellular ROS for normal cells (Control), H₂O₂-stimulated cells, and H₂O₂-stimulated cells after treatment with 20 μM of Rhe or H-RMM in a) L929 and b) MC3T3 fibroblast cell lines.

References

1. J. Zheng, R. Fan, H. Wu, H. Yao, Y. Yan, J. Liu, L. Ran, Z. Sun, L. Yi, L. Dang, P. Gan, P. Zheng, T. Yang, Y. Zhang, T. Tang and Y. Wang, *Nat. Commun.*, 2019, **10**, 1604.
2. L. M. Young, J. C. Saunders, R. A. Mahood, C. H. Revill, R. J. Foster, L.-H. Tu, D. P. Raleigh, S. E. Radford and A. E. Ashcroft, *Nat. Chem.*, 2015, **7**, 73-81.
3. H. Yao, K. Domoto, T. Isohashi and K. Kimura, *Langmuir*, 2005, **21**, 1067-1073.
4. I. Irwansyah, Y. Li, W. Shi, D. Qi, W. R. Leow, M. B. Y. Tang, S. Li and X. Chen, *Adv. Mater.*, 2015, **27**, 648-654.
5. W. J. E. M. Habraken, J. Tao, L. J. Brylka, H. Friedrich, L. Bertinetti, A. S. Schenk, A. Verch, V. Dmitrovic, P. H. H. Bomans, P. M. Frederik, J. Laven, P. van der Schoot, B. Aichmayer, G. de With, J. J. DeYoreo and N. A. J. M. Sommerdijk, *Nat. Commun.*, 2013, **4**, 1507.
6. T. Xu, C. Liang, D. Zheng, X. Yan, Y. Chen, Y. Chen, X. Li, Y. Shi, L. Wang and Z. Yang, *Nanoscale*, 2020, **12**, 15275-15282.